6-7-2019

Toward the Ultrasonic Sensing of Organic Carbon in Seagrass-Bearing Sediments

Gabriel R. Venegas
University of Texas at Austin

Abdullah Rahman
The University of Texas Rio Grande Valley, Abdullah.Rahman@utrgv.edu

Kevin M. Lee
University of Texas at Austin

Megan S. Ballard
University of Texas at Austin

Preston S. Wilson
University of Texas at Austin

Geophysical Research Letters

RESEARCH LETTER
10.1029/2019GL082745

Toward the Ultrasonic Sensing of Organic Carbon in Seagrass-Bearing Sediments

G. R. Venegas[1,2], A. F. Rahman[3], K. M. Lee[1], M. S. Ballard[1], and P. S. Wilson[1,2]

[1]Applied Research Laboratories, University of Texas at Austin, Austin, TX, USA, [2]Walker Department of Mechanical Engineering, University of Texas at Austin, Austin, TX, USA, [3]School of Earth, Environmental, and Marine Sciences, University of Texas Rio Grande Valley, Brownsville, TX, USA

Key Points:
- Seagrass-bearing sediment *P* wave modulus correlated better with organic carbon content than with mud content
- Presence of organic carbon between grains can affect bulk wave propagation
- Ex situ results show promise for rapid in situ organic carbon estimation within the studied seagrass meadow

Correspondence to:
G. R. Venegas,
gvenegas@arlut.utexas.edu

Citation:
Venegas, G. R., Rahman, A. F., Lee, K. M., Ballard, M. S., & Wilson, P. S. (2019). Toward the ultrasonic sensing of organic carbon in seagrass-bearing sediments. *Geophysical Research Letters*, *46*, 5968–5977. https://doi.org/10.1029/2019GL082745

Received 7 MAR 2019
Accepted 9 MAY 2019
Accepted article online 16 MAY 2019
Published online 7 JUN 2019

Abstract Ten percent of all organic carbon (C_{org}) absorbed by the ocean each year is stored in seagrass-bearing sediments. The preservation of these carbon stores is considered a vital method to mitigate climate change. Seagrass-bearing sediments have been correlated with sediment geophysical properties yet have not been related to sediment acoustic properties. For this purpose, sediment cores were collected from a *Thalassia testudinum* seagrass meadow in South Texas, USA, where geophysical, acoustical, and C_{org} properties were measured. It is hypothesized that when deposits of C_{org} adsorb onto mineral surfaces and are stored in pore spaces, compliant layers between grain contacts and the formation of an organic-rich suspension reduce sediment stiffness. Results from this seagrass meadow demonstrated a strong correlation between sediment *P* wave modulus and C_{org} and show promise toward the development of an in situ ultrasonic sediment probe to more rapidly quantify and monitor seagrass carbon stores.

1. Introduction

Seagrass meadows form the foundation of many shallow water coastal ecosystems across the globe by providing nursery and foraging grounds (Whitfield, 2017), sediment stabilization (Ginsburg & Lowenstam, 1958; Scoffin, 1970), nutrient cycling (McGlathery et al., 2007), and production and storage of organic carbon (C_{org}; Duarte et al., 2005). Seagrasses occupy less than 0.2% of the world's oceans but contribute to 10% of oceanic C_{org} burial Duarte et al. (2005), with about twice the average C_{org} storage per hectare (ha) as terrestrial soils (Fourqurean et al., 2012). Seagrasses are among the world's most valuable organic carbon ecosystems estimated at $1.9 trillion annually but are rapidly disappearing due to destructive fishing practices, boat propellers, coastal engineering, nutrient and sediment pollution, and climate change (Waycott et al., 2009). Carbon storage in the top meter of seagrass-bearing sediments is equivalent to an estimated 520 Mg eq/ha of CO_2 (Pendleton et al., 2012). When seagrasses are degraded, lost, or converted to other land uses, their large carbon stores are exposed and ultimately released into the atmosphere as CO_2. Hence, protecting these carbon stores is recognized as an important step toward mitigating anthropogenic greenhouse gas emissions (Mcleod et al., 2011; Pendleton et al., 2012).

Uncertainties in the estimates of carbon sequestered within seagrass meadows hinder the development of monitoring, recording, and verification frameworks for organic carbon climate mitigation projects. The most recent comprehensive compilation of data, from 946 distinct sites across the world, presented two ranges of estimates for C_{org} stock of global seagrasses: 4.2 to 8.4 or 9.8 to 19.8 Pg C, depending on the methodology used for sediment C_{org} estimation (Fourqurean et al., 2012). So for each methodology, there is an uncertainty of a factor of 2 in these estimates. One major reason for this uncertainty is that the total area of global seagrass coverage is poorly known (Chmura et al., 2014). Another reason for the uncertainty is that seagrass carbon pools are generally estimated from point-based sediment core sampling spatially extrapolated statistically across seagrass meadows (Howard et al., 2014). Core sampling of underwater seagrass-bearing sediments is a difficult, labor-intensive, and time-consuming process. Subsequent laboratory processing of the sediment samples and the elemental analysis of C_{org} are also time consuming and expensive. These hurdles limit the number of seagrass sediment cores taken from this ecosystem and thus contribute to the continuation of uncertainties in the estimates of C_{org} in global seagrass meadows (Mcleod et al., 2011).

Studies have demonstrated the potential for in situ measurements of various soil characteristics, such as water content, salinity, temperature, and nutrient status, using the dielectric, magnetic, and acoustic

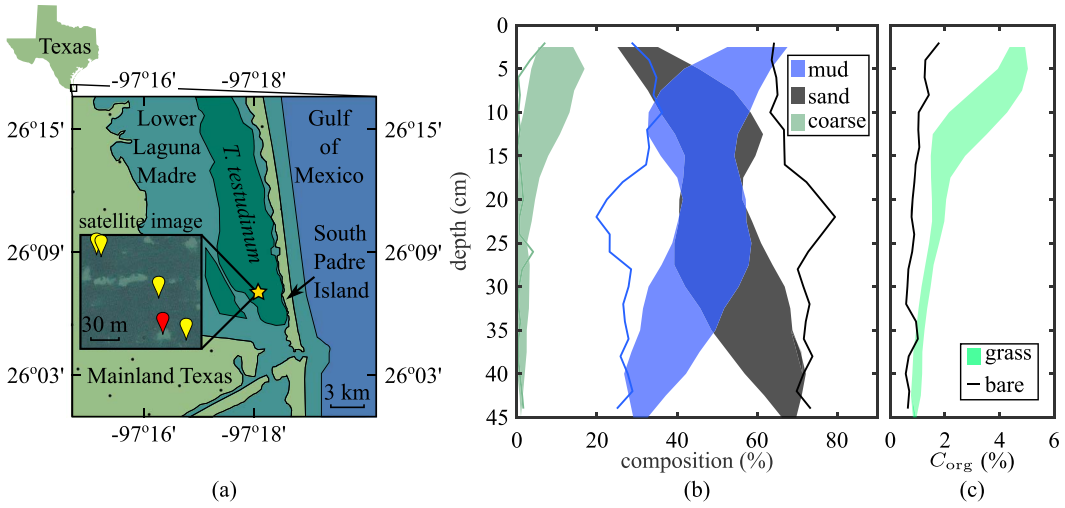

Figure 1. (a) Experiment site marked with a yellow star. Dark green regions represent the *Thalassia testudinum* meadow. Expanded region shows the locations of the four seagrass cores (yellow pins) and one bare patch core (red pin). Sediment composition (b) and C_{org} (c) depth profiles for the seagrass cores (shaded regions) and for the bare patch core (lines). Shaded regions represent a standard deviation about the mean, depth averaged in 5-cm bins. Since only one bare sediment core was collected, no spread was reported.

properties of soil (Brutsaert & Luthin, 1964; Doolittle & Brevik, 2014; Flammer et al., 2001; Topp et al., 1980). But to date, there is no published study on estimating soil carbon using the transmission of acoustic or electromagnetic energy through the soil media. The only reliable methods of estimating soil carbon are laboratory-based methods of combustion or elemental analysis.

Recent outcomes have demonstrated that there is a well-correlated relationship between the C_{org} stored in seagrass-bearing sediment and various sediment properties such as density, grain size, and porosity (Dahl et al., 2016; Rohr et al., 2016; Serrano et al., 2016). These findings are consistent with the literature that have shown how fine-grain mineral particles, such as silt and clay, bind to organic material to form complex, porous, low-density sediment fabrics (Bennett et al., 1991) and protect the trapped organic matter (OM) within small pore spaces from microbial decomposition. These same bulk sediment properties have been shown to measurably affect how sound propagates through marine sediment (Jackson & Richardson, 1991; Marion et al., 1992), but these effects have been mainly attributed to the inorganic mineral constituents that make up marine sediment. How OM affects sediment acoustic properties remains less studied requiring further investigation.

The development of a portable, nondestructive, and reliable acoustic method for estimating soil carbon would be a significant step toward easily assessing sediment C_{org} in situ and thus decreasing the uncertainties in the estimates of C_{org} in global seagrass meadows. The objective of this study is to first explore the relationship between C_{org} and sediment acoustic properties using established methods. To this end, sediment cores from a field experiment in a shallow coastal seagrass meadow were studied. The transmission characteristics of ultrasonic waves were measured along with other bulk sediment properties and compared with C_{org}.

2. Materials and Methods

A field experiment was conducted in the Lower Laguna Madre, located on the southern Gulf of Mexico coast of Texas, USA, between the mainland and the barrier South Padre Island (Figure 1a). The Lower Laguna Madre is one of five hypersaline coastal ecosystems in the world (Javor, 1989) and contains no river inlets. The experimental site consisted of a *Thalassia testudinum* seagrass meadow, had an average water depth of 1 m, and had a tidal range of 0.35 m. The seagrass meadow covers roughly 65% of the lagoon and accounts for 75% of seagrass cover along the Texas coast (Onuf, 2007). Four seagrass-bearing sediment cores and one bare-patch sediment core (free from seagrass cover) were extracted from the experimental site by driving 7.85-cm-diameter, 0.2-cm-wall-thickness polyvinyl chloride tubes into the bay floor via manual percussion.

Figure 1a marks the locations from where the seagrass and bare patch cores were extracted. Once inserted into the sediment, each core was capped at the top and removed slowly with a hand-cranked winch. The bottom of the core was capped underwater to avoid air entrapment in the sample. Cores were stored vertically on the boat under shade until they were transferred to the shore-based laboratory for analysis.

2.1. Acoustical Analysis

Cores were maintained vertical in the laboratory at 24 °C and were scanned with a Core And Resonance Logger (CARL; Venegas et al., 2017) within 24 hr of extraction. For this study, CARL measured sound speed and attenuation across the diameter of the core in 2-cm vertical increments downward from the water-sediment interface.

To measure the sound speed in each core, 20-μs-long tone bursts were generated at 300 kHz. The signal was amplified and transduced from the projector into a compressional wave that traveled radially through the sample to the opposite side of the core, where it was measured by the receiver. Transducers were acoustically coupled to the core walls using oil-filled core logger transducers with a resonance at 250 kHz. The received signal was conditioned, acquired, and averaged on an oscilloscope. The received tone bursts were digitally filtered 10% above and below the center frequency of the tone burst. A reference core filled with degassed fresh water of known sound speed c_w (Coppens, 1981) was used to calibrate the measurement system. The time difference Δt was found by locating the time delay associated with the peak of the cross-correlation function between the received signals through the reference and sample cores. The sound speed in the sediment core was calculated using

$$c_{sed} = \frac{c_w}{1 - c_w \frac{\Delta t}{d_i}}, \tag{1}$$

where d_i is the inner diameter of the core liner (Jackson & Richardson, 1991).

For this work, only sound speeds measured at 300 kHz are reported. At lower frequencies near or below the acoustic resonance of the gas volumes encapsulated in the plant tissue or free bubbles in the sediment itself due to anaerobic decomposition (DOE, 2008; Howard et al., 2014), sound speed is more sensitive to bubble size and volume fraction of gas than the C_{org} of the sediment (Dogan et al., 2017; Lee et al., 2017). Also, when the sediment particle size is on the order of or larger than the acoustic wavelength, known as the region of multiple scattering, there is large attenuation of acoustic waves and a dramatic drop in sound speed (Argo et al., 2011; Kimura, 2011; Yang & Seong, 2018) independent of the C_{org} sequestered in the sediment. The ratio of mean grain diameter to acoustic wavelength remained within 0.002–0.034 for this study. Encapsulated bubbles with resonances higher than 300 kHz or coarser sediment fragments could result in unaccounted experimental uncertainty. This uncertainty, however, was identified by a bimodal cross correlation between the received signal through the reference material and through the sample. In these cases, special care was taken to insure the data analysis algorithm picked the peak corresponding with the earlier direct arrival through the sediment phase, rather than the slower scattered arrival.

2.2. Sediment Properties

After the acoustic measurements were completed, the cores were vertically preserved in a freezer and sliced in the same increments scanned by CARL. By freezing the cores, samples confined within the polyvinyl chloride core liner could be sliced cleanly without significantly altering the sediment structure. The water-sediment interface was marked before freezing to account for any potential expansion, and only a negligible amount of expansion was observed. The dimensions and weight of each sediment slice were recorded to calculate the frozen bulk density as the frozen weight divided by the volume it occupied. The slices were placed in an oven at 65 °C for 3–4 days until their dry weight reached an equilibrium value that was recorded and divided by the volume to determine the dry bulk density ρ_{dry}. Porosity β was then calculated using

$$\beta = \frac{m_{frozen} - m_{dry}}{\rho_{ice} V}, \tag{2}$$

where m_{frozen} and m_{dry} are the frozen and dried mass of the slice, respectively, ρ_{ice} is the density of ice, and V is the volume of the slice. Frozen density values were corrected to the ambient temperature of the laboratory, where the cores were acoustically logged by

$$\rho_{wet} = \frac{m_{dry} + \beta V \rho_{water}}{V}, \tag{3}$$

where ρ_{wet} is the corrected sediment wet bulk density, and ρ_{water} is the water density at 24 °C. Depending upon the calculated porosity, corrected wet density values were 1–6% greater than the frozen density values.

Since the sound speed of a material is a function of both its density and stiffness, the primary wave (*P* wave) modulus was reported in order to remove the interdependence sound speed has with density. The *P* wave modulus (M) is the dynamic (acoustic) and frequency-dependent stiffness sensed by a compressional wave (Mavko et al., 2009) and is defined as

$$M = \rho_{wet} c_{sed}^2, \tag{4}$$

where c_{sed} is the sound speed of the sediment. The M can also be expressed in terms of the bulk modulus K and shear modulus G and is $M = K + \frac{4}{3}G$. However, since the shear wave speed was not measured, it was not possible to isolate K and G, and hence they were combined into the same effective stiffness variable.

Sediment particle-size distribution was determined using a laser-diffraction particle-size analyzer for all particles smaller than 500 μm, and a dry sieving technique was used for larger particles. In preparation for particle size analysis, a 10-g subsample of the dried sediment was wet-sieved through a 500-μm sieve to minimize fine particles adhering to larger particles to help control measurement bias. Both coarse and fine particles were dried in the same manner. Dried coarse particles were vibrated and sorted through a stack of 710-, 1,000-, 2,000-, and 2,800-μm sieves. Dried fine particles were gently homogenized with a mortar and pestle and sprinkled into a dispersant unit, where they were dispersed for 4 min with an ultrasonic in-line sonicator set to maximum power to insure adequate particle dispersion and analyzed (Ryżak & Bieganowski, 2011). Cumulative distribution functions from both coarse and fine particles were combined proportionally to their recorded dry mass and used to compute grain size statistics (Folk & Ward, 1957). Mud content (MC) is defined explicitly as the sum of both clay and silt-sized particles according to the Wentworth Scale (Wentworth, 1922) and was computed from the cumulative distribution functions evaluated at 62.5 μm for every sample slice. Sand content was similarly computed and defined as any particle larger than 62.5 μm and smaller than 2 mm (Wentworth, 1922). Coarse particles larger than 2 mm mainly consisted of shell hash and carbonate fragments.

2.3. Organic Carbon Content

The remaining unsorted dried sample was then homogenized gently with a mortar and pestle and passed through a 63-μm sieve. A 0.5-g subsample from the fines were placed on a ceramic crucible and into a muffle furnace heated to 500 °C for 4 hr. This process volatilized all the C_{org} and other organic materials in the sample. Then 5 mg of the ash containing the inorganic carbon (C_{inorg}) among other inorganic materials was placed into an elemental analyzer. The C_{inorg} was determined by taking the postmuffled to premuffled weight ratio and multiplying it by the percent carbon content of the ash. The total percent carbon content of the sample was recorded by placing 5 mg of the fines directly into the elemental analyzer. The C_{org} was then calculated by subtracting the C_{inorg} from the total carbon content (Howard et al., 2014). The C_{org} values are thus estimated from the particles less than 63 μm in size and presented as a percentage of the dry mass of each 2-cm core section.

3. Results

Significant differences in all measured sediment parameters were observed between the cores taken from an area containing seagrass compared with the core taken from the bare patch. Figures 1b and 1c show sediment composition separated into composition and C_{org}, respectively. Compared to the bare sediment, the seagrass-bearing sediment contained more C_{org}, more coarse particles such as plant litter, shell hash, and carbonate fragments, along with greater MC. These constituents resulted in sediment with higher porosity, lower density, and lower stiffness. In the seagrass cores near the water-sediment interface, MC as much as 70% and C_{org} values as high as 6% were found, whereas 45 cm below the water-sediment interface, 20% MC was reported with C_{org} values as low as 0.5% by dry mass. In this study, organic carbon content acquired from both seagrass and bare patches were consistent with literature values from the same site to within the 90% confidence intervals reported in Figure 22 in Greene (2017).

The relationship between M and ρ_{wet} was used to identify two regimes plotted in Figure 2a. Sediment with lower M and ρ_{wet} values followed a line of constant sound speed (isovelocity) equal to that of the seawater, until M surpassed a threshold of 4.2 GPa (stiffness dominated). This threshold was used to distinguish

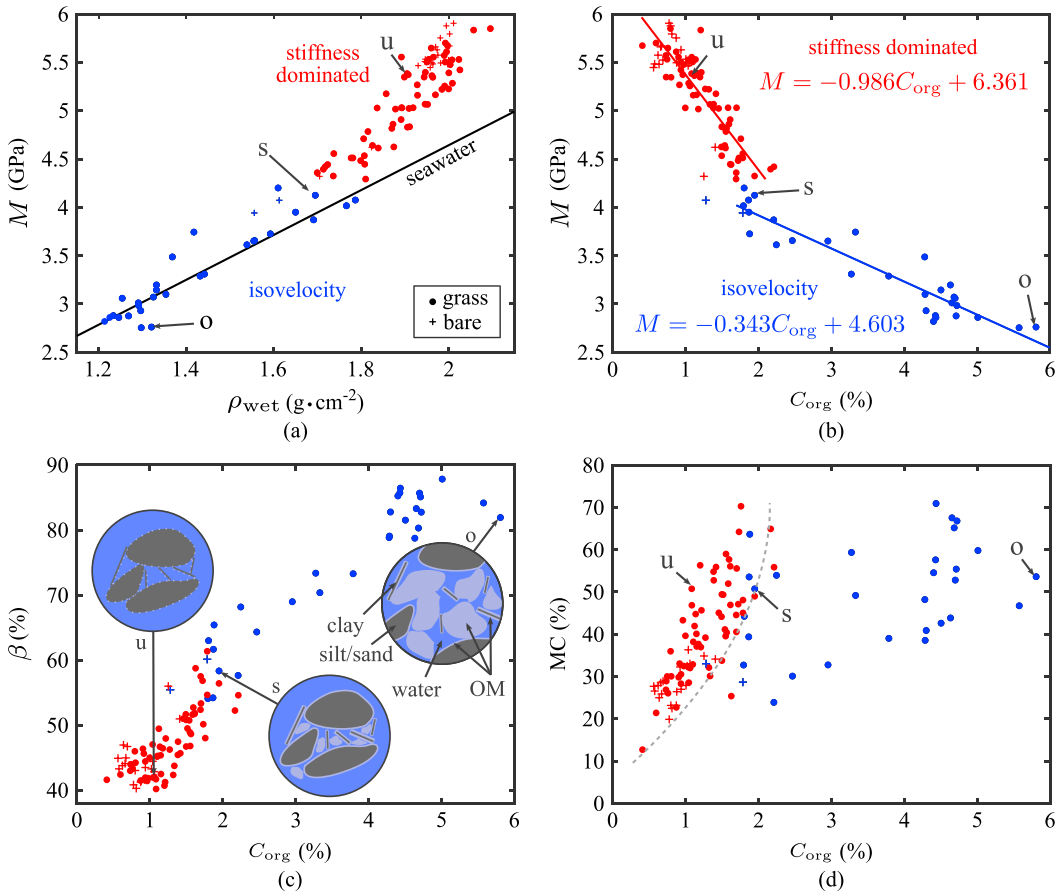

Figure 2. (a) Stiffness-mass relationship distinguishes isovelocity regime (blue points) from stiffness-dominated regime (red points). Line of constant sound speed equal to seawater (black line) is plotted using equation (4). Data taken from seagrass and bare cores are represented as dots and crosses, respectively. (b) M showed a strong correlation with C_{org} in both regimes. Linear regressions on seagrass-bearing sediment in isovelocity (blue line) and stiffness-dominated (red line) are plotted. (c) β and (d) MC were also compared with C_{org}. Gray dashed line represents refractory background level. Qualitative illustrations of three sediments with equal MC, undersaturated (u), saturated (s), and oversaturated (o) with C_{org} are shown. MC = mud content; OM = organic matter.

between the isovelocity regime and the stiffness-dominated regime. The depth at which this threshold occurred varied between 10 and 20 cm into the sediment. For the remainder of the paper, sediment property comparisons will be performed within these respective regimes.

Pearson correlation coefficients (r values) were determined and tabulated for the following sediment properties: MC, C_{org}, ρ_{dry}, β, and M (Table 1). Since MC, ρ_{dry}, and β have been shown to be good predictors of C_{org} (Dahl et al., 2016), they were chosen as candidate parameters to compare with M of the sediment. Two r values were found between each parameter. The top values within each cell correspond with data in the isovelocity regime, while the bottom values correspond with data in the stiffness-dominated regime. Off-diagonal elements contain a number of asterisks pertaining to a p value range defined as the probability of attaining at least the corresponding r value under the null hypothesis.

In the stiffness-dominated regime, all sediment parameters, particularly M, correlated well to C_{org} with p values less than 0.001. Porosity and MC were positively correlated with C_{org}, while ρ_{dry} and M were negatively correlated with C_{org}. In this regime, M correlated well with all sediment properties except MC. In the isovelocity regime, there was an overall higher correlation of C_{org} to all sediment properties with the exception of MC, and like in the stiffness-dominated regime, C_{org} correlated best with M. The highest r values reported in the isovelocity regime, however, were observed when comparing M and ρ_{dry} with β. The only sediment properties that correlated well with MC was C_{org} in the stiffness-dominated regime. Though all

Table 1
Pearson Correlation Coefficients (r Values)

	MC (%)	C_{org} (%)	ρ_{dry} (g/cm^2)	β (%)	M (GPa)
MC (%)		0.39	−0.52	0.54	−0.46
		0.74	−0.55	0.44	−0.55
C_{org} (%)	*		−0.93	0.93	−0.94
	**		−0.84	0.78	−0.88
ρ_{dry} (g/cm^2)	*	**		−0.997	0.94
	**	**		−0.90	0.92
β (%)	*	**	**		−0.95
	**	**	**		−0.81
M (GPa)	*	**	**	**	
	**	**	**	**	

Note. Top right triangle: r values between variables determined from all seagrass cores within isovelocity (top) and stiffness-dominated (bottom) regimes. Bottom left triangle: Cross-diagonal elements represent p values for corresponding r values. MC = mud content.

correlations with MC in the isovelocity regime were statistically significant, corresponding p values were consistently greater than 0.001.

A line of best fit was plotted showing the trend of M as a function of C_{org} for each regime (Figure 2b). Empirical regressions were performed only on the seagrass-bearing sediment cores (denoted by dots), although data points from the bare patch sediment core are also shown in the figure as crosses. Equations for empirical regressions displayed in Figure 2b are

$$M = -0.986C_{org} + 6.361 \tag{5}$$

and

$$M = -0.343C_{org} + 4.603 \tag{6}$$

for the stiffness-dominated and isovelocity regimes, respectively, where M has units of gigapascals. The regimes identified in Figure 2b are similarly separated into two unique linear regimes when comparing M with C_{org}. The transition between the two regimes occurred at a C_{org} value of roughly 1.8% and was also identified by a 0.5-GPa reduction in M. This reduction in acoustic stiffness coincided with a 10% increase in β shown in Figure 2c. There was a distinct positive, linear relationship between MC and C_{org} in the stiffness-dominated regime that spanned the entire range of MC measured in this data set (Figure 2d). A gray dashed line is depicted to separate the stiffness-dominated and isovelocity regimes. When transitioning into the isovelocity regime, the data became scattered spanning a similar range of MC seen in the stiffness-dominated regime.

To demonstrate the effect C_{org} has on sediment properties, three seagrass-bearing sediment samples with comparable MC, undersaturated (u), saturated (s), and oversaturated (o) with C_{org}, are identified in Figures 2a–2d and depicted in Figure 2c. Although the mineral contents of the three samples were comparable, the sediment behaved significantly differently. Transitioning from the undersaturated to saturated states, a 23% reduction in M and an 11% reduction in ρ_{wet} was observed, while β increased 16%. When transitioning from the saturated to oversaturated states, a 33% reduction in M and a 22% reduction in ρ_{wet} was observed, while β increased by 24%.

4. Discussion

The purpose of this work is to better understand the relationship between independent variables that constitute the sediment, such as MC and C_{org}, and dependent variables, such as M, ρ_{dry}, and β. The r values from Table 1 show an expected interdependence among dependent variables, since the minerals are denser and stiffer than water or the OM. For example, to first order, the more porous the sediment, the fewer minerals are contained within a unit volume, and the less dense and less stiff the sediment becomes. However,

it is the sediment constituents that ultimately control β. Although M correlates well with ρ_{dry} and β, M is also ultimately controlled by the sediment constituents. Based on the results of this study, observations reported in the sedimentology literature, and established models for sound propagation in granular media, two separate physical mechanisms are postulated to explain the dependence between M and C_{org} in the stiffness-dominated and isovelocity regimes, respectively.

Within the stiffness-dominated regime, as C_{org} increases, small deposits of OM begin to absorb onto mineral surfaces (Figure 2c [u]; Mayer, 1999; Mayer et al., 1993; 2004), which create compliant layers between the otherwise stiffer frame composed of grain-to-grain contacts, thereby reducing M. Ransom et al. (1997) observed patches of OM adsorbed onto mineral surfaces with transmission electron microscopy (TEM), though how this phenomenon affects bulk sediment properties was not addressed by his work. Sound propagation in consolidated granular sediments have been successfully modeled as slip-stick processes between neighboring grain micro-asperities separated by very thin interstitial seawater (Buckingham, 2000). The contact area referred to in this framework is precisely where organic matter is most protected from decomposition (Mayer et al., 2004) and can therefore affect bulk wave propagation.

Once a threshold is reached where mineral surfaces and pores spaces become saturated with OM (Figure 2c [s]), the grain-to-grain slip-stick processes that contribute to the overall sediment stiffness begin to diminish, as the grains begin to separate. This transition is represented in Figure 2b by a 0.5-GPa reduction in stiffness and in Figure 2c by a 10% increase in porosity. This saturation point is posed to be equivalent to the C_{org} "refractory background level" (Berner, 1982; Henrichs & Reeburgh, 1987) and related to the mineral surface area (Mayer, 1994). Many experimental sites included in Mayer (1994) showed values of C_{org} consistent with that of the transition region of this study. Mayer et al. (1993) claims that adsorption of C_{org} onto mineral surfaces is the dominant mechanism that drives long-term C_{org} sequestration in marine sediment. However, due to the presence of the aboveground and belowground biomass to help stabilize the sediment, seagrass-bearing sediments can sequester above the refractory background level.

Once the majority of the grains are separated by interstitial OM, a low-density organic-rich suspension of minerals is formed, described by the isovelocity regime and depicted in Figure 2c (o). The suspension of minerals by C_{org} has been observed in natural fine-grained sediments with TEM (Furukawa et al., 2009). In this regime, the behavior is described by the well-understood suspension theory, where both density and stiffness of the suspension are controlled by the volume fraction of the substrate and the minerals using a mixture law, described in Urick (1947). In the case of seagrass-bearing sediment, the substrate consists of a water-saturated lignin-rich organic slurry originating mostly from digested plant litter (Peduzzi & Herndl, 1991). In the isovelocity regime, the fibrous C_{org} slurry prevents the minerals from settling and maintains the sediment in a highly porous state. As C_{org} increases, the volume fraction of the slurry also increases, causing M and ρ_{wet} to decrease. Suspension theory and the r values from Table 1 both suggest that, in the isovelocity regime, β, which is dependent on C_{org}, controls both M and ρ_{dry}. More controlled studies are required to test this hypothesis and address if or where these two regimes exist across different sediment types or different seagrass species. However, this phase change represented by the organic-rich isovelocity regime found within the top 20 cm of sediment appears to be less dependent upon sediment type (Figure 2d) and could potentially be applied to isovelocity regimes located in different seagrass meadows.

The MC of sediment has been shown to increase β, which in turn can decrease M and ρ_{wet} (Jackson & Richardson, 1991; Marion et al., 1992) and could be another factor attributing to the decrease in M, independent of C_{org}. Although a negative trend between M and MC was observed (Table 1), Pearson correlation coefficients suggest that within the *T. testudinum* seagrass meadow studied, it was the organic material that played the dominated role in controlling M and ρ_{dry} in both regimes. The presence of fine-grained minerals, however, is closely related to C_{org} content (Anderson, 1988; Oades, 1988; Tiessen et al., 1984) due to the increase in mineral surface area (Mayer, 1994). In fact, Curry et al. (2007) directly observed two mechanisms that preserve OM from digestion in fine-grained sediments using TEM: OM adsorption onto mineral surfaces and encapsulation within small pores of the sediment microfabric that were inaccessible to enzymes used in the study. These observations in the microscale are consistent with data reported within the stiffness-dominated regime, shown in Figure 2d, where the relationship between MC and C_{org} closely resembles the surface area to C_{org} relationship reported in Figure 2 in Mayer (1994). However, once the saturation point is surpassed in the isovelocity regime, OM is no longer protected from microbial attack by the fine-grained minerals and becomes weakly correlated with MC. In support of this, Mayer et al. (1993) stated

that low-density organic particles cannot account for grain size dependence of bulk C_{org} in a continental shelf region. The weak correlation to MC in the isovelocity regime is evidence that much of the C_{org} in the upper carbon-rich layer is low-density OM.

5. Conclusion

Sediment-sequestered C_{org} ranging from 0.5% to 6% by dry mass of the *T. testudinum* seagrass meadow in the Lower Laguna Madre correlated best with M compared to other sediment properties such as MC, ρ_{dry}, and β. Since the Lower Laguna Madre is predominately composed of fine sand with a high M, the reduction in stiffness observed when the seagrass meadow incorporates its organic-rich sludge in the sediment provided a measurable contrast that can be detected via acoustical means. Although seagrasses more commonly grow in sandy sediments, seagrasses that grow in silt or clay deposits with MC greater than 70% may provide a less detectable contrast in M with the background sediment due to the presence of C_{org}. However, the background sediments with high MC could still yield high C_{org} due to an inherently larger refractory background level.

While the methods reported here are ex situ, the strong correlation between M and C_{org} demonstrated in this study shows promise toward the development of an acoustic in situ sediment probe that, when inserted into the sediment, could instantaneously measure M, without the need for the collection and postprocessing of sediment samples. An instantaneous method to estimate the depth dependence of seagrass-bearing sediment C_{org} does not exist and has the potential to rapidly sample large areas at finer spatial and depth resolutions. Such a tool could capture finer-scale heterogeneities and facilitate studies on spatiotemporal changes in organic carbon stocks due to environmental and anthropogenic stressors. This method, however, requires the correlation between M and C_{org} to be consistent across different seagrass meadows and sediment types. Although larger-scale studies have already demonstrated that the correlations between MC, ρ_{dry}, and β with C_{org} are consistent across multiple European *Zostera marina* seagrass meadows (Dahl et al., 2016), more investigation is required to assess the feasibility of applying this method in situ and to different seagrass meadows and sediment types. If the M-C_{org} relationship is not consistent among different sites, a set of calibration measurements would be required to determine a site-specific correlation, which would be used to estimate C_{org} across the entire meadow. In addition, the operating frequency of the sediment probe would need to be higher than the resonances of the gas voids in the belowground biomass to accurately measure M. This frequency is typically higher than the operating frequencies of most commercial sonars. Since sediment attenuation scales with frequency, propagation paths at this frequency must also be short, on the order of those performed with CARL. For these reasons, a physical sediment probe must be inserted into the sediment to overcome the short acoustic penetration depths that would otherwise confound the use of downward looking sonars for this application.

Acknowledgments
Field data are archived in Open Science Framework (https://osf.io/e5jga/). This work was funded by the Office of Naval Research and the Applied Research Laboratories Independent Research and Development Program. The authors thank Kelly Dorgan for insightful conversations regarding this topic; Allen Reed for providing core logger transducers; and Aslan Aslan, Ivy Hinson, Sarah Fernandez de la Vega, and Kimbell Bui for their assistance with the extraction and processing of sediment cores.

References

Anderson, D. (1988). The effect of parent material and soil development on nutrient cycling in temperate ecosystems. *Biogeochemistry*, *5*, 71–97.

Argo, T. F., Guild, M. D., Wilson, P. S., Schröter, M., Radin, C., & Swinney, H. L. (2011). Sound speed in water-saturated glass beads as a function of frequency and porosity. *Journal of the Acoustical Society of America*, *129*, EL101–EL107.

Bennett, R. H., Bryant, W. R., & Hulbert, M. H. (1991). *Microstructure of fine-grained sediments: From mud to shale*. New York: Springer-Verlag. Frontiers in Sedimentary Geology.

Berner, R. A. (1982). Burial of organic carbon and pyrite sulfur in the modern ocean: Its geochemical and environmental significance. *American Journal of Science*, *282*, 451–473.

Brutsaert, W., & Luthin, J. N. (1964). The velocity of sound in soils near the surface as a function of the moisture content. *Journal of Geophysical Research*, *69*, 643–652.

Buckingham, M. J. (2000). Wave propagation, stress relaxation, and grain-to-grain shearing in saturated, unconsolidated marine sediments. *Journal of the Acoustical Society of America*, *108*, 2796–2815.

Chmura, G., Short, F., Torio, D., Arroya-Mora, P., Fajardo, P., Hatvany, M., & van Ardenne, L. (2014). North America's blue carbon: Assessing seagrass, salt marsh and mangrove carbon sinks a final report (Tech. Rep.): Montreal, Canada: Commission for Environmental Cooperation.

Coppens, A. B. (1981). Simple equations for the speed of sound in Neptunian waters. *Journal of the Acoustical Society of America*, *69*, 862–863.

Curry, K. J., Bennett, R. H., Mayer, L. M., Curry, A., Abril, M., Biesiot, P. M., & Hulbert, M. H. (2007). Direct visualization of clay microfabric signatures driving organic matter preservation in fine-grained sediment. *Geochimica et Cosmochimica Acta*, *71*, 1709–1720.

DOE, U. (2008). Carbon cycling and biosequestration: Report from the March 2008 Workshop (*Tech. Rep.*): DOE/SC-108, US Department of Energy Office of Science.

Dahl, M., Deyanova, D., Gütschow, S., Asplund, M. E., Lyimo, L. D., Karamfilov, V., et al. (2016). Sediment properties as important predictors of carbon storage in Zostera marina meadows: A comparison of four European areas. *PLOS ONE*, *11*, e0167493.

Dogan, H., White, P. R., & Leighton, T. G. (2017). Acoustic wave propagation in gassy porous marine sediments: The rheological and the elastic effects. *Journal of the Acoustical Society of America*, *141*, 2277–2288.
Doolittle, J. A., & Brevik, E. C. (2014). The use of electromagnetic induction techniques in soils studies. *Geoderma*, *223*, 33–45.
Duarte, C. M., Middelburg, J. J., & Caraco, N. (2005). Major role of marine vegetation on the oceanic carbon cycle. *Biogeosciences*, *2*, 1–8.
Flammer, I., Blum, A., Leiser, A., & Germann, P. (2001). Acoustic assessment of flow patterns in unsaturated soil. *Journal of Applied Geophysics*, *46*, 115–128.
Folk, R., & Ward, W. (1957). Brazos River bar: A study of the significance of grain size parameters. *Journal of Sedimentary Research*, *27*, 3–26.
Fourqurean, J. W., Duarte, C. M., Kennedy, H., Marb, N., Holmer, M., Mateo, M. A., et al. (2012). Seagrass ecosystems as a globally significant carbon stock. *Nature Geoscience*, *5*, 505–509.
Furukawa, Y., Watkins, J. L., Kim, J., Curry, K. J., & Bennett, R. H. (2009). Aggregation of montmorillonite and organic matter in aqueous media containing artificial seawater. *Geochemical Transactions*, *10*, 1–11.
Ginsburg, R. N., & Lowenstam, H. A. (1958). The influence of marine bottom communities on the depositional environment of sediments. *The Journal of Geology*, *66*, 310–318.
Greene, A. L. (2017). Applications of side scan and parametric echosounders for mapping shallow seagrass habitats and their associated organic carbon (Master's thesis). Retrieved from [ProQuest Dissertations and Theses]. (Order No. 10263707).
Henrichs, S. M., & Reeburgh, W. S. (1987). Anaerobic mineralization of marine sediment organic matter: Rates and the role of anaerobic processes in the oceanic carbon economy. *Geomicrobiology Journal*, *5*, 191–237.
Howard, J., Hoyt, S., Isensee, K., Pidgeon, E., & Telszewski, E. (Eds.) (2014). Coastal blue carbon: Methods for assessing carbon stocks and emissions factors in mangroves,tidal salt marshes, and seagrass meadows. Conservation International, Intergovernmental Oceanographic Commission of UNESCO, International Union for Conservation of Nature, Arlington, VA, USA.
Jackson, D. R., & Richardson, M. D. (1991). *High-frequency seafloor acoustics*. New York: Springer.
Javor, B. (1989). *Hypersaline environments: Microbiology and biogeochemistry*. New York: Springer-Verlag.
Kimura, M. (2011). Velocity dispersion and attenuation in granular marine sediments: Comparison of measurements with predictions using acoustic models. *Journal of the Acoustical Society of America*, *129*, 3544–3561.
Lee, K. M., Ballard, M. S., McNeese, A. R., & Wilson, P. S. (2017). Sound speed and attenuation measurements within a seagrass meadow from the water column into the seabed. *Journal of the Acoustical Society of America*, *141*, EL402–EL406.
Marion, D., Nur, A., Yin, H., & Han, D. (1992). Compressional velocity and porosity in sand-clay mixtures. *Geophysics*, *57*, 554–563.
Mavko, G., Mukerji, T., & Dvorkin, J. (2009). *The rock physics handbook: Tools for seismic analysis of porous media*. Cambridge: Cambridge University Press.
Mayer, L. M. (1994). Surface area control of organic carbon accumulation in continental shelf sediments. *Geochimica et Cosmochimica Acta*, *58*, 1271–1284.
Mayer, L. M. (1999). Extent of coverage of mineral surfaces by organic matter in marine sediments. *Geochimica et Cosmochimica Acta*, *63*, 207–215.
Mayer, L. M., Jumars, P. A., Taghon, G. L., Macko, S. A., & Trumbore, S. (1993). Low-density particles as potential nitrogenous foods for benthos. *Journal of Marine Research*, *51*, 373–389.
Mayer, L. M., Schick, L. L., Hardy, K. R., Wagai, R., & McCarthy, J. (2004). Organic matter in small mesopores in sediments and soils. *Geochimica et Cosmochimica Acta*, *19*, 3863–3872.
McGlathery, K. J., Sundbäck, K., & Anderson, I. C. (2007). Eutrophication in shallow coastal bays and lagoons: The role of plants in the coastal filter. *Marine Ecology Progress Series*, *348*, 1–18.
Mcleod, E., Chmura, G. L., Bouillon, S., Salm, R., Björk, M., Duarte, C. M., et al. (2011). A blueprint for blue carbon: Toward an improved understanding of the role of vegetated coastal habitats in sequestering CO_2. *Frontiers in Ecology and the Environment*, *10*, 552–560.
Oades, J. (1988). The retention of organic matter in soils. *Biogeochemistry*, *5*, 35–70.
Onuf, C. P. (2007). Laguna Madre: Seagrass status and trends in the northern Gulf of Mexico: 1940–2002: U.S. Geological Survey Scientific Investigations Report 2006-5287. (p. 267).
Peduzzi, P., & Herndl, G. J. (1991). Decomposition and significance of seagrass leaf litter (*Cymodocea nodosa*) for the microbial food web in coastal waters (Gulf of Trieste, Northern Adriatic Sea). *Marine Ecology Progress Series*, *71*, 163–174.
Pendleton, L., Donato, D. C., Murray, B. C., Crooks, S., Jenkins, W. A., Sifleet, S., et al. (2012). Estimating global blue carbon emissions from conversion and degradation of vegetated coastal ecosystems. *PLOS ONE*, *7*, e43542.
Ransom, B., Bennett, R., Baerwald, R., & Shea, K (1997). TEM study of in situ organic matter on continental margins: Occurrence and the monolayer hypothesis. *Marine Geology*, *138*, 1–9.
Rohr, M. E., Bostrom, C., Canal-Vergés, P., & Holmer, M. (2016). Blue carbon stocks in Baltic Sea eelgrass (*Zostera marina*) meadows. *Biogeosciences*, *13*, 6139–6153.
Ryżak, M., & Bieganowski, A. (2011). Methodological aspects of determining soil particle-size distribution using the laser diffraction method. *Journal of Plant Nutrition and Soil Science*, *174*, 624–633.
Scoffin, T. P. (1970). The trapping and binding of subtidal carbonate sediments by marine vegetation in Bimini Lagoon, Bahamas. *Journal of Sedimentary Research*, *40*, 249–273.
Serrano, O., Lavery, P., Duarte, C. M., Kendrick, G. A., Calfat, A. M., York, P. H., et al. (2016). Can mud (silt and clay) concentration be used to predict soil organic carbon content within seagrass ecosystems?. *Biogeosciences*, *13*, 4915–4926.
Tiessen, H, Stewart, J., & Hunt, H. (1984). Concepts of soil organic matter transformations in relation to organo-mineral particle size fractions. *Plant Soil*, *76*, 287–295.
Topp, G. C., Davis, J., & Annan, A. P. (1980). Electromagnetic determination of soil water content: Measurements in coaxial transmission lines. *Water Resources Research*, *16*, 574–582.
Urick, R. (1947). A sound velocity method for determining the compressibility of finely divided substances. *Journal of Applied Physics*, *18*, 983–987.
Venegas, G. R., Wilson, P. S., Lee, K. M., Ballard, M. S., McNeese, A. R., & Dorgan, K. M. (2017). Core and Resonance Logger (CARL) measurements of fine-grained sediments containing infauna. *Proceedings of Meetings on Acoustics*, *31*, 005001.
Waycott, M., Duarte, C. M., Carruthers, T. J. B., Orth, R. J., Dennison, W. C., & Olyarnik, S. (2009). Accelerating loss of seagrasses across the globe threatens coastal ecosystems. *Proceedings of the National Academy of Sciences of the United States of America*, *106*, 12,377–12,381.
Wentworth, C. K. (1922). A scale of grade and class terms for clastic sediments. *The Journal of Geology*, *30*, 377–392.
Whitfield, A. K. (2017). The role of seagrass meadows, mangrove forests, salt marshes and reed beds as nursery areas and food sources for fishes in estuaries. *Rev. Fish. Biol. Fisher.*, *27*, 75–110.

Yang, H., & Seong, W. (2018). High frequency compressional wave speed and attenuation measurements in water-saturated granular media with unimodal and bimodal grain size distributions. *Journal of the Acoustical Society of America*, *143*, 659–665.